Supporting Information

One-photo excitation pathway in 2D in-plane heterostructure for effective visible-light-driven photocatalytic degradation

Mengchi Liu, Yiwen Cheng, Yuee Xie, Yingcong Wei, Jinhui Xing, Yuanping Chen*, Jing Xu*

School of Physics and Electronic Engineering, Jiangsu University, Zhenjiang, Jiangsu, 212013, P. R. China

*Corresponding author. E-mail: xjing@ujs.edu.cn (J. Xu); chenyp@ujs.edu.cn (Y.P. Chen).

Experiment and test details

1. Synthesis of BiOCl

The BiOCl was synthesized by hydrothermal method. Usually, 3 mmol of $Bi(NO_3)_3 \cdot 5H_2O$ and 3 mmol of NH_4Cl were dissolved in 80 mL of deionized water. After stirring in the air for 30 min, the reaction mixture was sealed in a 100 mL polytetrafluoroethylene-lined autoclave and heated at 120 °C for 24 h. Then, the product was washed three times with deionized water and dried at 60 °C.

2. Characterizations

Powder X-ray diffraction (XRD) patterns of the samples were carried on an X-ray diffractometer (Bruker D2 Phaser) with Cu Kα radiation (λ = 1.5418 Å). Scanning electron microscopy (SEM) images were obtained on JZEISS SUPRA 55 compact instruments. Transmission electron microscopy (TEM) images and EDS mapping were obtained on a Thermo Fisher Scientific microscope (JEM-2100). X-ray photoelectron spectra (XPS) were taken on Thermo Scientific K-Alpha instrument using Al Kα radiation. Ultraviolet-visible diffuse reflectance spectra (DRS) spectra of the prepared samples were obtained by a UV-vis spectrometer (UV2600, Shimadzu, Japan). The photoluminescence spectra (PL) were obtained using a JASCO FP-6500 fluorescence spectrophotometer. All photoelectrochemical properties including the electrochemical impedance spectra (EIS), transient photocurrent response, and Mott-Schottky (M-S) curves were measured on an electrochemical workstation (CHI660B) using a three-electrode system with the platinum plate as the counter electrode and Ag/AgCl as the reference electrode used in 0.1 M Na_2SO_4 solution. Electron spin resonance (ESR, ER200-SRC) spectra were obtained on an electron paramagnetic resonance spectrometer (Bruker EMX PLUS).

3. DFT calculation

The calculations were carried out by the Vienna ab initio Simulation

Package (VASP) based on density functional theory (DFT) [1]. PBE exchange-correlation functional based on generalized gradient approximation (GGA) was used for structural optimization and electronic structure calculation [2]. The default plane-wave cutoff energy was set at 400 eV. The electron energy is calculated using a 21×21×1 k-point mesh. The convergence criterion is set to be 10-5 eV. These structures relax completely until the force of all atoms is less than 10−3 eV/Å. The DFT-D2 method is used to correct the interlayer Van der Waals (VDW) interaction [3].

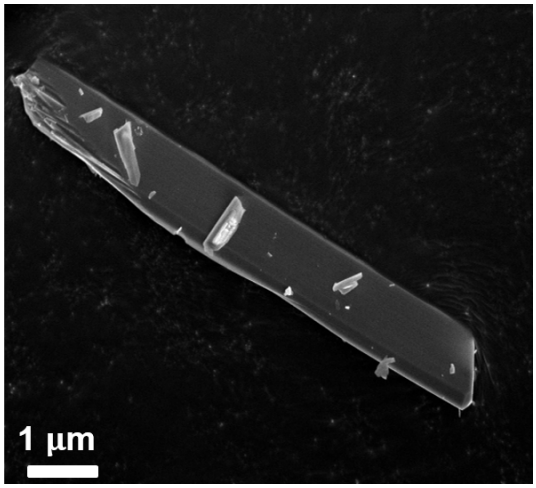

Fig. S1. The SEM image of CAU-17.

Table S1. Atomic proportion and mass proportion of three elements

Z	Element	Atomic Fraction (%)	Mass Fraction (%)
83	Bi	24.42	76.73
8	O	58.16	13.99
17	Cl	17.41	9.28

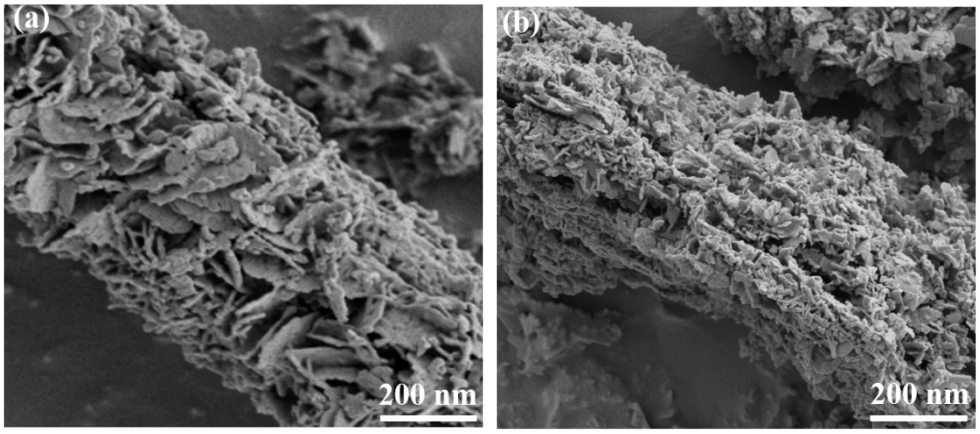

Fig. S2 The SEM images of i-I (a) and i-Br (b).

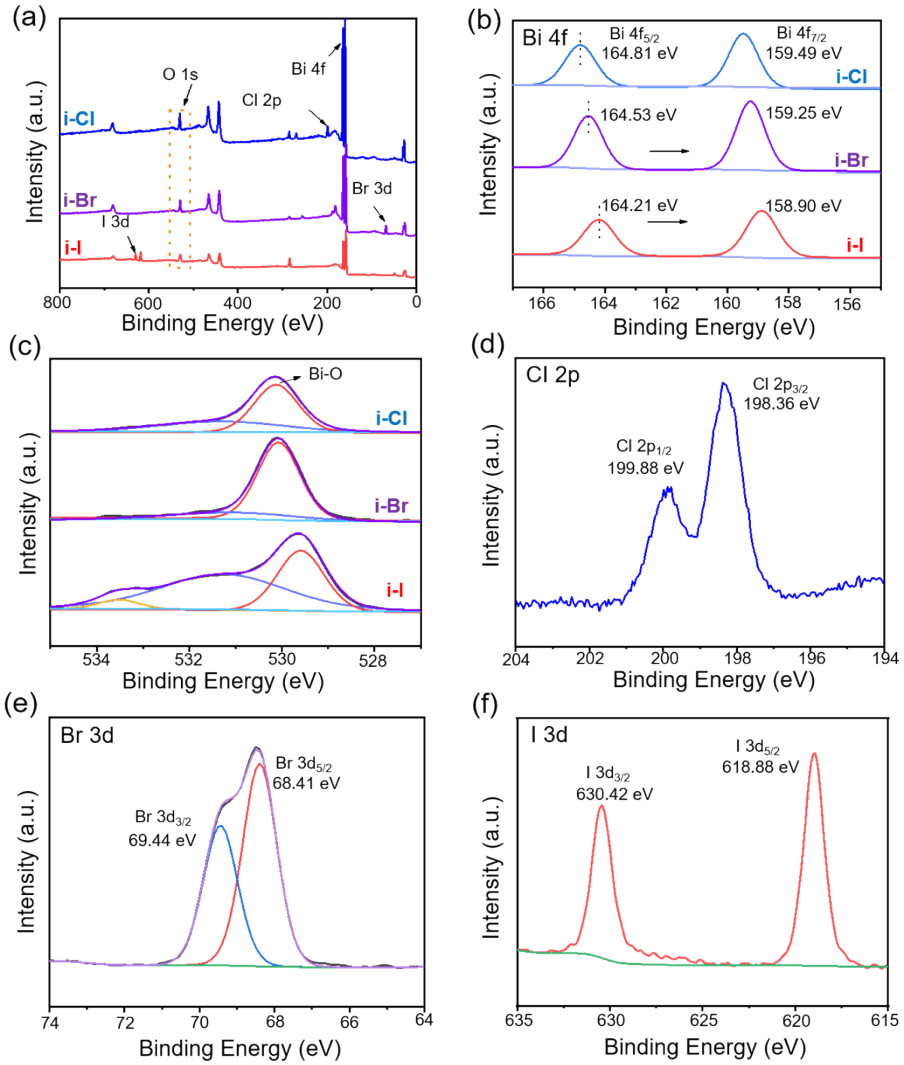

Fig. S3. XPS survey spectra of i-X samples (a); High-resolution spectrum of Bi 4f (b), O 1s (c), Cl 2p (d), Br 3d (e), I 3d (f).

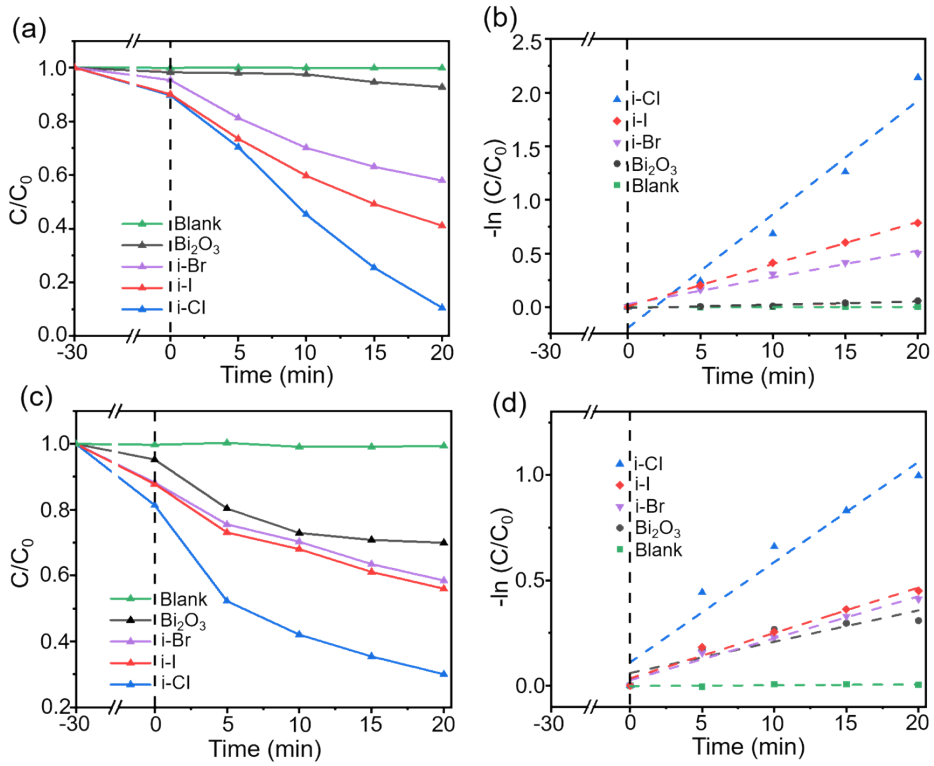

Fig. S4. The photocatalytic RhB degradation performance (a) and the quasi-first-order kinetics linear fitting diagram (b) of i-X (X = Cl, Br, I) samples; The photocatalytic TC degradation performance and the quasi-first-order kinetics linear fitting diagram (d) of i-X (X = Cl, Br, I) samples.

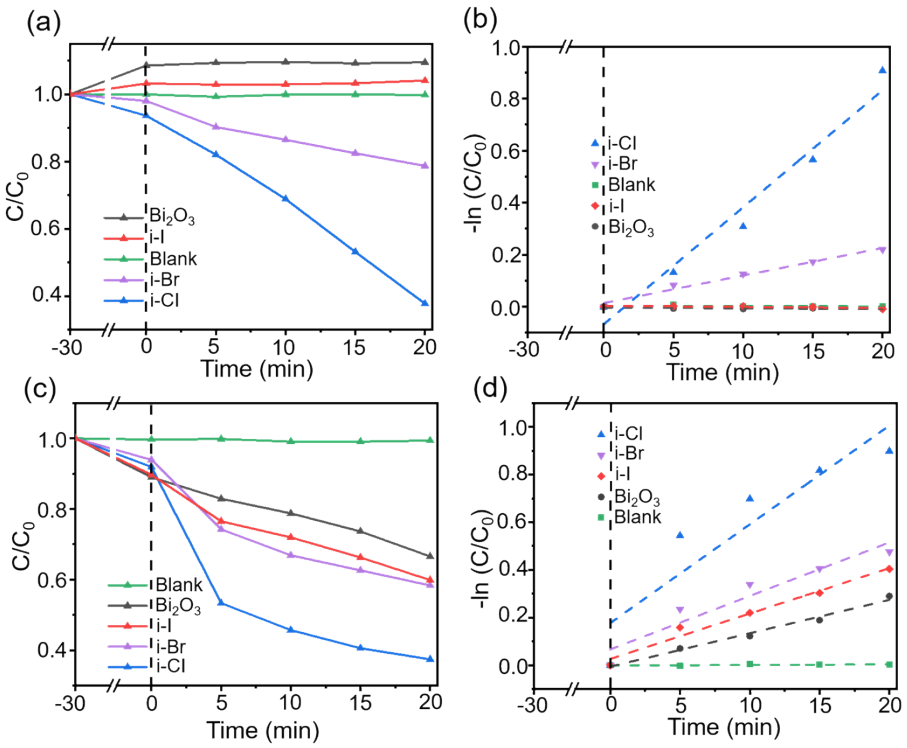

Fig. S5. The photocatalytic RhB degradation performance (a) and the quasi-first-order kinetics linear fitting diagram (b) of i-X (X = Cl, Br, I) and Bi_2O_3 samples in mixed wastewater; The photocatalytic TC degradation performance and the quasi-first-order kinetics linear fitting diagram (d) of i-X (X = Cl, Br, I) and Bi_2O_3 samples in mixed wastewater.

Table S2. Photocatalytic performance for degrading RhB of BiOCl-based catalysts reported previously

Material	Irradiation	Sample amount (mg)	RhB (mg/L)	Irradiation time (min)	Degradation rate (%)	k	Refs.
i-Cl	Visible light	10	10	20	90	0.106	Herein
BiOCl/KTO	Visible light	50	10	90	100	0.055	4
GO/BiOCl/PAN	Visible light	20	8	90	38	-	5
BiOCl/TiO_2 on FTO	Visible light	3cm*7cm	2.5	180	99	0.043	6
BiOCl/$Bi_2O_2CO_3$	Visible light	20	20	60	99	-	7
BiOCl/$Bi_{24}O_{31}Br_{10}$	simulated sunlight	25	10	90	98	0.035	8
BiOCl/CQDs	Visible light	20	10	40	98	0.092	9
WO_3/ BiOCl/$BiVO_4$	Visible light	25	10	120	75	0.010	10
BiOCl/$H^+Ti_2NbO_7^-$	Visible light	100	20	90	98	0.060	11

Table S3. Photocatalytic performance for degrading TC of BiOCl-based catalysts reported previously

Material	Irradiation	Sample amount (mg)	TC (mg/L)	Irradiation time (min)	Degradation rate (%)	k	Refs.
i-Cl	Visible light	10	10	20	70	0.048	Herein
Ag/BiOCl/diatomite	Visible light	30	10	60	86	0.025	12
BiOCl/$K^+Ca_2Nb_3O_{10}^-$	simulated sunlight	35	35	150	94	0.016	13
BiOCl-BMO	Visible light	50	10	100	97	-	14
BiOCl@CeO_2	Visible light	50	10	120	90	0.015	15
BiOCl/Cu_2O	Visible light	20	20	80	90	0.015	16
Fe_3O_4/BiOCl/BiOI	simulated sunlight	20	40	80	89	0.019	17

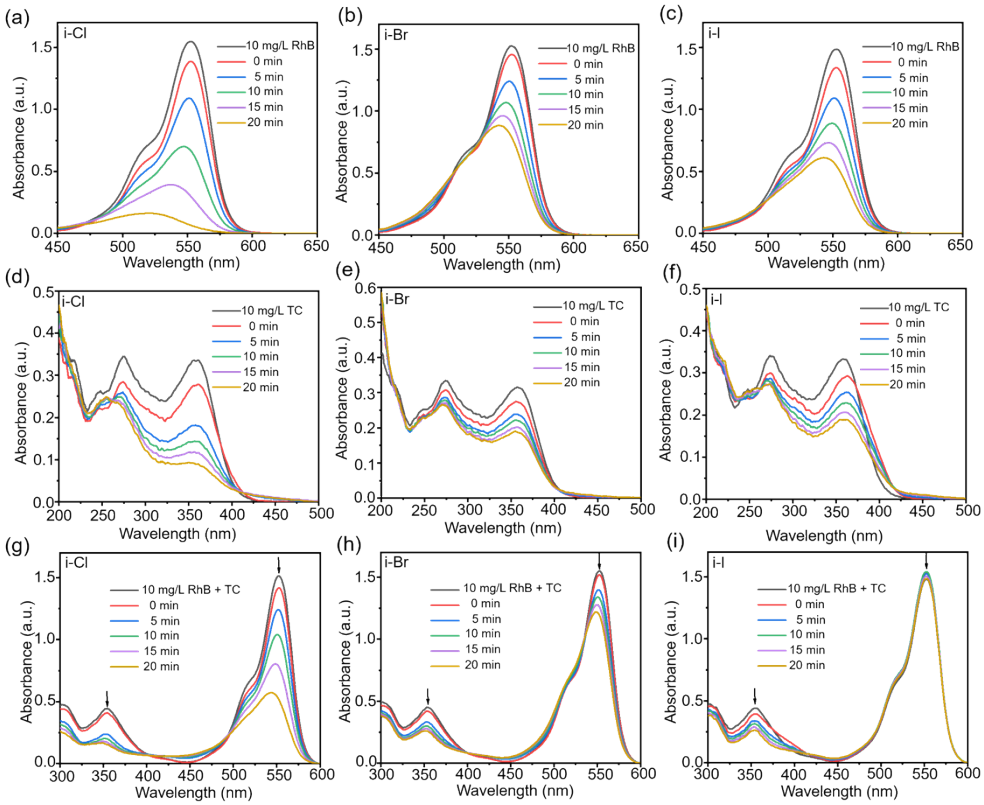

Fig. S6. UV-Vis curves of RhB solution (a, b, c), TC solution (d, e, f), and mixed wastewater with RhB and TC (g, h, i).

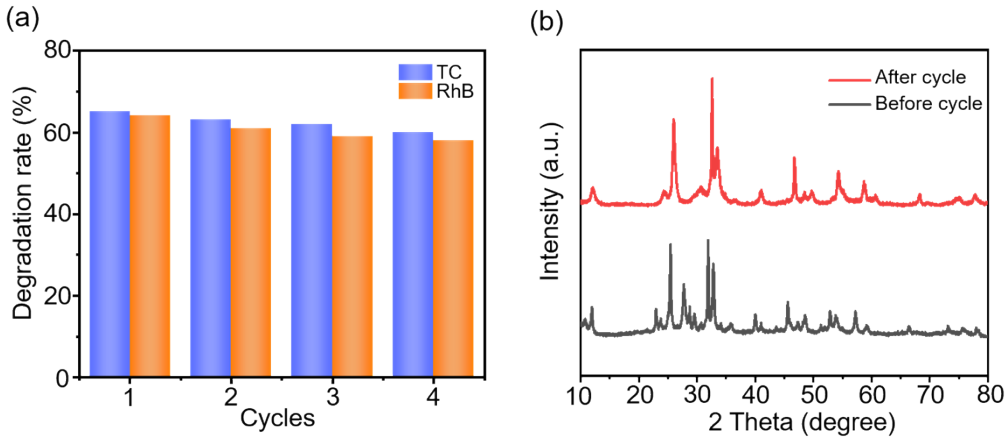

Fig. S7. The cycling experiments results (a) and XRD patterns before and after recycling process (b) of i-CI for mixed wastewater degradation.

References

[1] Kresse G, Furthmüller J. Efficiency of ab-initio total energy calculations for metals and semiconductors using a plane-wave basis set. Computat Mater Sci, 1996, 6, 15-50

[2] Kresse G, Furthmüller J. Efficient iterative schemes for ab initio total-energy calculations using a plane-wave basis set. Phys Rev B, 1996, 54, 11169

[3] Grimme S, Antony J, Ehrlich S, et al. A consistent and accurate ab initio parametrization of density functional dispersion correction (DFT-D) for the 94 elements H-Pu. J Chem Phys, 2010, 132, 154104

[4] Durai M, Chauhan D, Durai M, et al. Layered KTO/BiOCl nanostructures for the efficient visible light photocatalytic degradation of harmful dyes. Chemosphere, 2022, 306, 135659

[5] Zhang Y, Park M, Kim H Y, et al. In-situ synthesis of graphene oxide/BiOCl heterostructured nanofibers for visible-light photocatalytic investigation. J Alloy Compd, 2016, 686, 106-114

[6] Shen Y H, Yu X Y, Lin W T, et al. A facile preparation of immobilized BiOCl nanosheets/TiO_2 arrays on FTO with enhanced photocatalytic activity and reusability. Appl Surf Sci, 2017, 399, 67-76

[7] Xie J, Guo N N, Liu A J, et al. Simple solid-state synthesis of BiOCl/$Bi_2O_2CO_3$ heterojunction and its excellent photocatalytic degradation of RhB. J Alloy Compd, 2019, 784, 377-385

[8] Li J J, Xiao X Y, Xiao Y, et al. Construction of Z-scheme BiOCl/$Bi_{24}O_{31}Br_{10}$ hierarchical heterostructures with enhanced photocatalytic activity. J Alloy Compd, 2022, 921, 166050

[9] Di J, Xia J X, Ji M X, et al. Carbon quantum dots modified BiOCl ultrathin nanosheets with enhanced molecular oxygen activation ability for broad spectrum photocatalytic properties and mechanism insight. ACS Appl Mater Inter, 2015, 7, 20111-20123

[10] Li H L, Chen Y J, Zhou W, et al. WO_3/$BiVO_4$/BiOCl porous nanosheet composites from a biomass template for photocatalytic organic pollutant degradation. J Alloy Compd, 2019, 802, 76-85

[11] Gao X, Feng Y, Dong P Y, et al. Rational design 2D/2D BiOCl/$H^+Ti_2NbO_7$-heterojunctions for enhanced photocatalytic degradation activity. Appl Surf Sci, 2020, 521, 146334

[12] Chen J, Ren Q F, Ding Y, et al. Synthesis of bifunctional composites Ag/BiOCl/diatomite: Degradation of tetracycline and evaluation of antimicrobial activity. J Environ Chem Eng, 2021, 9, 106476

[13] Liang X M, Zhang Y Q, Li D, et al. 2D/2D BiOCl/$K^+Ca_2Nb_3O_{10}$-heterostructure with Z-scheme charge carrier transfer pathways for tetracycline degradation under simulated solar light. Appl Surf Sci, 2019, 466, 863-873

[14] Qiu Y J, Lu J J, Yan Y J, et al. Bismuth molybdate photocatalyst for the efficient photocatalytic degradation of tetracycline in water under visible-light irradiation. Surf Interfaces, 2022, 31, 102009

[15] Wang H X, Liao B, Lu T, et al. Enhanced visible-light photocatalytic degradation of tetracycline by a novel hollow BiOCl@CeO_2 heterostructured microspheres: Structural characterization and reaction mechanism. J Hazard Mater, 2020, 385, 121552

[16] Yuan X X, Yang J Y, Yao Y Y, et al. Preparation, characterization and photodegradation mechanism of 0D/2D Cu_2O/BiOCl S-scheme heterojunction for efficient photodegradation of tetracycline. Sep Purif Technol, 2022, 291, 120965

[17] Dang J J, Guo J R, Wang L P, et al. Construction of Z-scheme Fe_3O_4/BiOCl/BiOI heterojunction with superior recyclability for improved photocatalytic activity towards tetracycline degradation. J Alloy Compd, 2022, 893, 162251